ACS MEASUREMENT SCIENCE Au
AN OPEN ACCESS JOURNAL OF THE AMERICAN CHEMICAL SOCIETY

pubs.acs.org/measureau
Article

Electrochemical Profiling of vWFA2 for Systemic Inflammatory State Detection

Bianca Elizabeth David,[§] Sasya Madhurantakam,[§] Jayanth Babu Karnam, Sriram Muthukumar, and Shalini Prasad*

Cite This: ACS Meas. Sci. Au 2024, 4, 721−728
Read Online
ACCESS | Metrics & More | Article Recommendations | Supporting Information

ABSTRACT: This research aims to develop a portable biosensor device for quickly detecting vWFA2, a biomarker for inflammatory conditions. This sensor could dramatically change detection methods and lead us to improve the sensitivity of our tests to overcome the limitations of conventional detection methods. Our label-free biomolecular assay is constructed on an Au-ZnO electrode surface and uses electrochemical impedance spectroscopy (EIS) to measure the capacitive change in impedance, revealing the binding effects of the target vWFA2, to the capture probe. Our developed biosensor platform exhibits greater sensitivity and specificity, covering a wide dynamic range of 750−24,000 pg/mL and showing a strong correlation with inflammatory conditions. This sensor exhibited a greater accuracy ranging from 86−110% for the known spiked concentrations in nondiluted or modified plasma samples. This electrochemical sensor has the potential to advance point-of-care diagnostic methods due to its high sensitivity and rapid response time. The vision behind this research is to develop an electrochemical sensor that can rapidly and accurately detect disease states, thus creating a pivotal prognostic tool in inflammatory state treatment and ultimately mitigating severe mortality and morbidity.

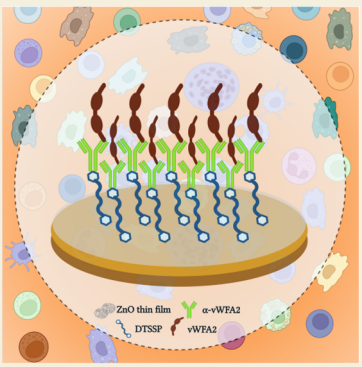

KEYWORDS: *biosensor, inflammation, biomarker, vWFA2, electrochemical, immunosensor*

INTRODUCTION

Life-threatening inflammatory conditions can arise from an attack on the systemic response of the human body by an infectious agent leading to clinical manifestations representing the imbalance between inflammation and coagulation. Disruption of the synergistic relationship between inflammation and coagulation can lead to fatal consequences, including microvascular damage and multiple organ failure in the form of a systemic inflammatory response.[1] Systemic inflammatory response syndrome (SIRS) is generally defined as a set of symptoms that occur after an infection and/or inflammatory state.[2] SIRS is manifested by nonspecific systemic symptoms such as hyper- or hypothermia, tachycardia, tachypnea and/or leukocytosis or leukopenia.[3] Other symptoms include mental confusion, hypotension, a decrease in urine output or unexplained thrombocytopenia.[4] Worsening of symptoms can lead to severe dysfunction and failure of major organ systems.[5] As the signs and symptoms are consistent with other inflammatory conditions, the overlap between the diseases is complicated by the vagueness of the presenting symptoms, leading to an inconclusive diagnosis and delay in treatment.[6] The systemic inflammatory state is potentially harmful, as life and death can be decided within minutes in the event of sepsis or septic shock. Several studies have investigated the role of biomarkers in diagnostics to reduce the delay time in inflammatory conditions. By closely monitoring progression, clinicians can detect the presence of inflammation, determine the severity, and initiate effective treatment.

Von willebrand factor (vWF), a large multimeric glycoprotein produced in the subendothelial matrix, undergoes intracellular processing, and glycosylation leading to multimer formation.[7] It circulates within blood plasma as a series of heterogeneous multimers and plays a critical role in physiologic hemostasis.[8] The interaction between vWF and glycoprotein receptors on exposed subendothelial fibrillar collagen triggers platelet migration to the injured site to form a platelet plug, ultimately arresting bleeding.[9] It also aids in the transport of clotting factors and induces amplification of the coagulation cascade.[10] The architecture of VWF is structured into four repeated domains assembled in the following order: D1-D2-D′-D3-A1-A2-A3-D4−C1−C2-C3−C4−C5-C6-CK, where D1-D2 represents the amino-terminal pro-peptide and the D′-CK portion represents the mature VWF subunit.[11] The A2 domain, known as vWFA2, is crucial in regulating vWF activity by acting as the mechanosensitive trigger that unfolds upon sheer vascular stress and exposes

Received: August 15, 2024
Revised: October 22, 2024
Accepted: October 24, 2024
Published: November 4, 2024

other domains.[12] This specific domain, vWFA2, is responsible for type 1 collagen binding via protease binding specificities and subsequent inflammatory reactions.[13] vWF in its polymeric form is a critical factor in coagulation via platelet adhesion but the specific substrate and receptor interactions within the subunit domains, such as vWFA2, are important.[14] The evidence indicating crosstalk between inflammation and coagulation, two critical systemic processes, is important to highlight as inflammation can activate the coagulation cascade while coagulation simultaneously spikes inflammatory activity.[15] Endothelial cells quickly respond to inflammatory stimuli by releasing vWF, triggering the host's acute phase response.[16] vWF responds to endothelial injury by mediating the adhesion between platelets and subendothelial components on sites of vascular injury via interactions between platelet membrane glycoproteins and exposed connective tissue components.[17] S. Figure 1 depicts the schematic representation of vWF binding to injured vascular subendothelial cells through specific glycoprotein receptor interactions. This binding interaction plays a crucial role in both platelet adhesion and aggregation.

vWFA2 was previously considered as an inflammatory marker in hemostatic pathologies, but its role in immune thrombosis is of great interest.[6] Decreased functionality of vWFA2 leads to severe hemorrhagic consequences as a result of the defective formation of platelet-rich thrombus and fibrin network.[18] Abnormally increased functionality of vWF is observed in systemic inflammation, making the marker crucial for assessing the severity of the disease.[19] The development of an assay utilizing vWFA2 could provide clinicians with a tool to rapidly initiate treatment for SIRS patients. Currently, there is little research on the role of vWFA2 in inflammatory diseases, as the marker has traditionally been studied in hemostatic diseases. As there is great interest in exploring the link between inflammation and coagulation, a sensor platform targeting vWFA2, a marker released in both systemic diseases, would help clinicians in patient stratification. There are no point-of-care prognostic devices for the detection of vWFA2 in inflammatory and very little research on electrochemical detection of this marker more broadly. The first prognostic device that could be used for disease classification and symptom management should be highly sensitive and have a wide dynamic range for its target marker. In the dynamic intersection of technologically advancing medicine and engineering, rapid diagnostic methods are essential for the prognostic evaluation of critically ill patients with clinical complications due to a dysregulated host response. As the paradigm of inflammatory pathogenesis is complex, various therapeutic approaches have been attempted using biomarkers as they contain important information to confirm the presence, absence, and severity of the condition. The evaluation of biomolecular markers in inflammatory conditions, especially in a systemic inflammatory response, is of utmost interest to develop an extremely rapid, robust, and immediately applicable diagnostic option.[20]

The current gold standard diagnostic method using blood cultures for accurate microbial diagnosis is associated with compromised sensitivity, prolonged processing time and a large sample volume required.[21] The development of a biosensor that can accurately detect the presence and concentration of a biomarker would allow clinicians to quickly act and create treatment plans. This research aims to develop and refine a novel point-of-care (POC) diagnostic device that enables the rapid detection of inflammatory biomarkers with a small sample volume for use in the clinical setting. The device consists of a disposable sensor cartridge connected to a portable electronic reader. It is functionalized to be highly sensitive for biomarker detection.[22] The electrode surface is prepared with specific capture probes for biomarker detection, fabricated on an electrode sensor array of nanofilm semiconductor material at the metal/electrode interface, and displayed on a computerized system.[22] Specifically, both the working electrode and reference electrode used were gold-plated sensor surfaces, modified with zinc oxide (ZnO) thin film, a semiconductor material with high excitation energy and wide band gap that improves sensor efficiency. Gold sensor surfaces are more popular in the biosensor world due to their biocompatibility, excellent conductivity, stability, useful electrical properties, and modification capabilities. ZnO was chosen as a semiconductor material due to its unique electrical properties which proved to enhance the electrochemical detection capabilities by increasing the surface coverage of the working electrode to accommodate higher antibody immobilization.[23,24]

The biosensor response is measured using electrochemical impedance spectroscopy. The specific aim of this research was to demonstrate the effectiveness of the proposed biosensor in improving diagnostic capabilities through a mechanistic approach to inflammatory biomarkers to aid disease detection for effective clinical management of inflammatory conditions.

MATERIALS AND METHODS

A specific recombinant human vWFA2 antibody and protein were purchased from R&D Systems. DTSSP (3,3′-dithiobis-(sulfosuccinimidyl propionate)) and PBS (Phosphate Buffer Saline) were obtained from Thermo Fisher Scientific. Healthy human lithium heparin (LiH) pooled plasma was acquired from Innovative Research, Inc., and used as such, without modification or dilutions. All proteins, antibodies, reagents, and pooled human plasma samples were stored according to their respective storage instructions until use. Each stock concentration was divided into smaller sample volumes to reduce the number of freeze−thaw cycles to a maximum of 3 cycles. The antibody was diluted in PBS, and the antigen concentrations were added to LiH pooled plasma to create a calibrated dose−response curve and to analyze other sensor properties.

Sensor Functionalization

The biosensor consists of a gold working electrode surrounded by a gold reference electrode. The surface of the working electrode was modified with zinc oxide (ZnO), a semiconducting layer to enhance the surface-to-volume ratio of the sensor.[25] The amount of reliable antibodies that needed to be loaded and the incubation time were also tested to determine variations in the impedance response between different incubation times of the antibodies. The ideal incubation time is designed to maximize response with minimal turnaround time for use in clinical settings with minimal turnaround time for use in clinical settings.

The immunoassay was functionalized on the electrode surface by preparing a cocktail solution containing DTSSP in phosphate buffer saline (PBS) and the anti-vWFA2 antibody total of 100 μL of the 10 mM DTSSP cocktail was allowed for successful conjugation of DTSSP with antibody for 30 min at room temperature under light protection before functionalization of the electrode surface. After incubation, 5 μL of the cocktail solution was manually added to immobilize the vWFA2 antibody-DTSSP cocktail on the surface of the working electrode and incubated for 30 min. Unbound cross-linkers and antibodies were removed by washing the electrode surface with PBS buffer solution. vWFA2 antigen dosage concentrations were prepared at 2-fold dilution in pooled human plasma. Figure 1 shows a schematic, step-by-step illustration of the mechanism of the functionalized biosensor, which can be used as a point-of-care

https://doi.org/10.1021/acsmeasuresciau.4c00060
ACS Meas. Sci. Au 2024, 4, 721−728

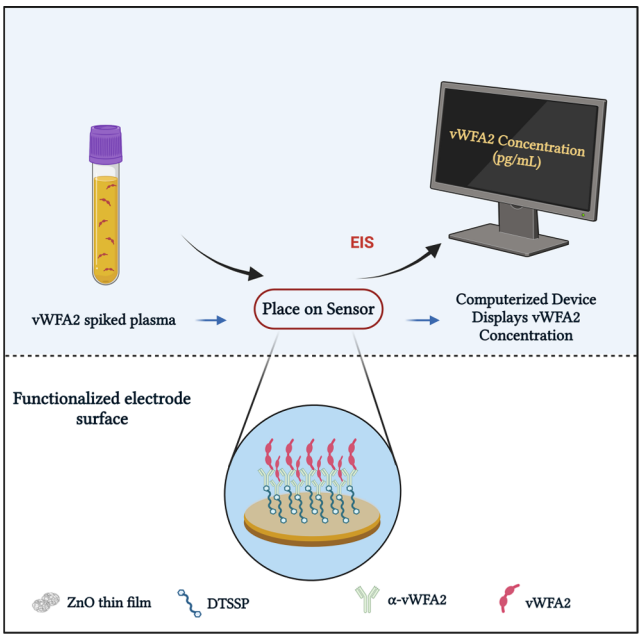

Figure 1. Schematic representation of the working mechanism of the developed biosensor as a point-of-care diagnostic device for the quantification of vWFA2 levels.

prediction device to quantify vWFA2 concentration. Sensor was calibrated using a wide range of vWFA2 concentrations in healthy human pooled plasma samples and recovery was evaluated from the calibration. Other biosensor properties such as accuracy, sensitivity, specificity, cross-reactivity, and variability were evaluated successfully in healthy human pooled plasma samples.

RESULTS AND DISCUSSION

The electrochemical performance of the point-of-care biosensing device was first validated using nonfaradaic electrochemical impedance spectroscopy (EIS) techniques for the detection of vWFA2 in pooled plasma samples. EIS is a powerful and versatile technique that is useful for analyzing features of electrochemical detection due to its nondestructive nature while maintaining coverage of a wide frequency range to provide quantitative analysis of the electrochemical behavior of a system.[26] The electrochemical performance of the functionalized biosensor was analyzed by measuring the resulting impedance response over a range of concentrations, spanning from the lowest to highest concentrations. The resulting impedance response plots, known as the Nyquist and Bode plots, help reinforce the sensitivity of the sensor platform to the biomarker concentration range.[27]

Impedance measurements were done over a range of frequencies spanning from 1 Hz to 1 MHz, increasing the dose concentrations of vWFA2 from 500 to 24,000 pg/mL and plotted Bode and Nyquist plots as shown in Figure 2. Figure 2a,b show the Bode of magnitude and phase angles across the entire frequency range and Figure 3b,d show the inset at lower frequency region. An increase in the Zmod and Zphase was seen with increasing the vWFA2 concentrations. While this displays a trend in the sensor performance with increasing WFA2 concentrations, the Nyquist plot (Figure 2c) confirms the biosensor behavior with vWFA2 doses. In a typical nonfaradaic Nyquist plot, the absence of redox material eliminated the dominance of charge transfer resistance with increasing dose concentrations. Similarly, solution resistance plays a major role in this kind of redox-free system with increasing doses and exhibits more noise than the signal to the captured protein. So, eliminating the effect of solution resistance is very crucial to check the original signal obtained toward the captured protein, particularly in protein-rich fluids such as plasma. As the Nyquist plot of a nonfaradaic system is represented by a continuous and incomplete semicircle, Figure 2c shows that with an increase in dose concentration, the radium of the curvature of the impedance curve also increases.[27] The higher concentration of vWFA2 leads to an increase in the resulting real impedance value, potentially due to the accumulation of the biomolecules in the electrical double layer, thus altering the conductivity of the solution (Figure 2c). The region shown in Figure 2c displays a decrease in the Zreal with increasing dose concentrations of vWA2 confirming the change in capacitance due to binding interactions between the vWFA2 antibody-to-antigen complex.

Levels of vWFA2 in infected patients range from a minimum of 300 pg/mL and span up to 50,000 pg/mL, thus it is vital to establish a biosensor with sensing capabilities to encompass this pathological range. Sensor functionality was evaluated by incrementally increasing dose concentrations, after functionalizing 10 μg/mL of antibody on the surface of the electrode. The incrementally increasing doses were tested to demonstrate a high sensitivity for vWFA2 in the wide dynamic range. This wide concentration range includes both healthy physiological levels and pathological elevations for flexible monitoring capabilities. Varying dose concentrations of vWFA2 were made in lithium-heparin pooled plasma to establish a CDR on the functionalized sensor within the detection range of 750–24,000 pg/mL. The incremental doses were prepared according to a 2-fold dilution, including 750, 1500, 3000, 6000, 12,000, and 24,000 pg/mL. An increase in the percent change to the baseline zero dose was observed with the incremental dose concentrations, from low to high. Figure 3a represents the significant difference seen between the lowest (750 pg/mL) and the highest (24,000 pg/mL) doses, with a regression coefficient value of 0.96. Figure 3b illustrates a box plot distribution of the calibrated dose responses within the same corresponding range, confirming a high affinity of the antibody to the antigen. This robust response provides evidence for capable detection methods for physiological and pathological levels of the vWFA2 biomarker.

After establishing the reliability of the calibrated dose responses' reliability, we evaluated the sensing platform's accuracy by conducting spike and recovery studies. This was carried out by spiking a known concentration of vWFA2 antigen onto the sensor and assessing the percentage response to measure the unknown concentrations as shown in Figure 4a. Range of vWFA2 concentrations 500, 1000, 2000, 4000, 8000, and 16,000 pg/mL were diluted in pooled plasma and tested using the sensor as shown in Figure 4b. The spiked concentrations were estimated from the calibrated dose–response curve in pooled plasma and then compared to the recovered concentration to evaluate the sensor's accuracy. The recovered concentrations were plotted on the *y*-axis against the spiked concentrations on the *x*-axis, as illustrated in Figure 4b. The recovered concentration of vWFA2 in plasma provided a regression coefficient of 0.99 (Figure 4b), confirming the biosensor's ability to accurately estimate the spiked concentrations of vWFA2 from the plasma samples. Additionally, Figure 4c illustrates a Pearson's correlation of 0.99, between the spiked concentrations and recovered concentrations

https://doi.org/10.1021/acsmeasuresciau.4c00060
ACS Meas. Sci. Au 2024, 4, 721–728

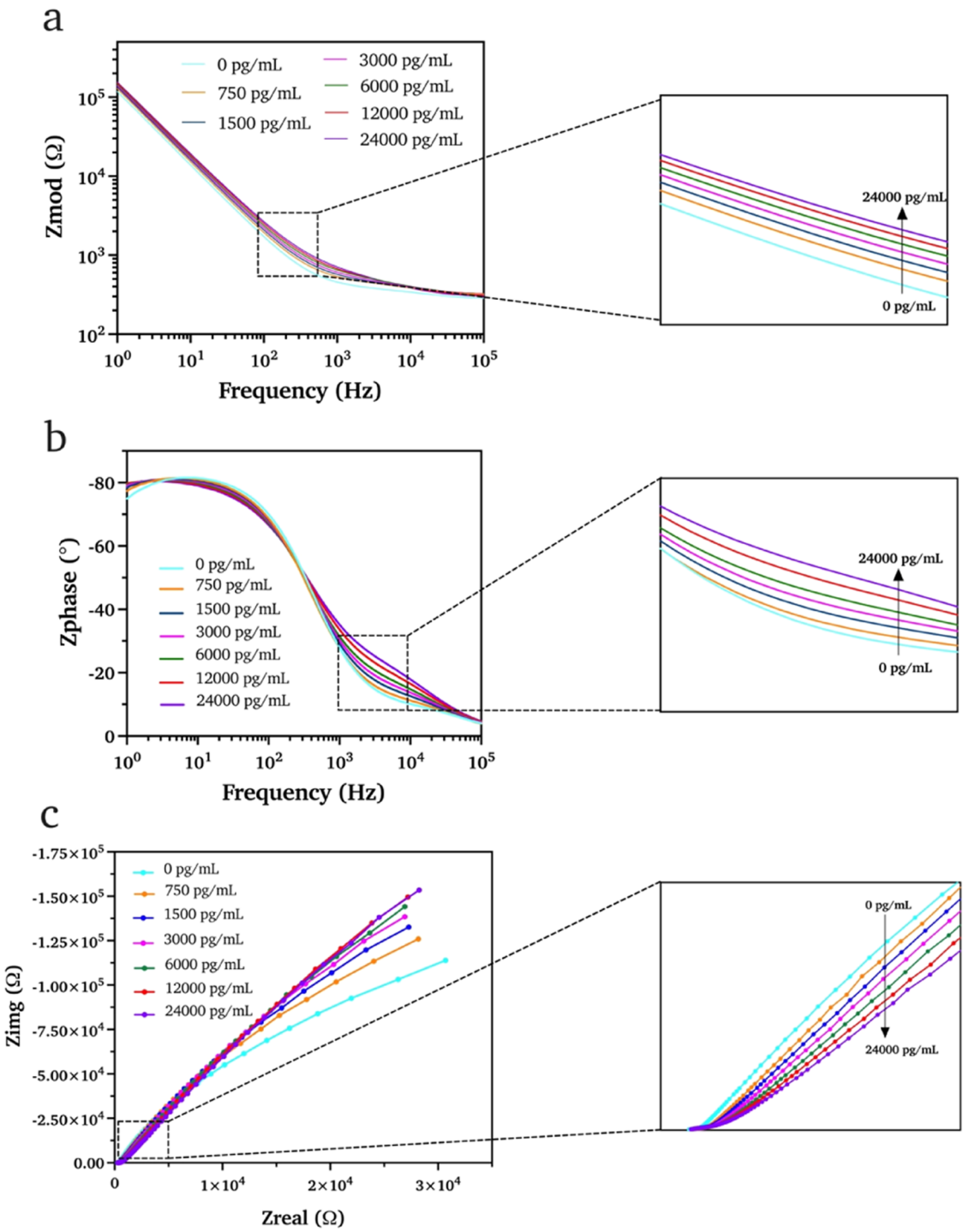

Figure 2. Bode (magnitude) (a), Bode (phase) (b), and Nyquist (c) plots representing impedance measurements at each concentration of vWFA2 in pooled plasma samples.

calculated using the calibrated dose−response curve (Figure 5).

One of the main goals of biosensor engineering is to achieve high sensitivity. To verify this, it is crucial to test the biosensor's specificity by examining its reaction to other potentially cross-reactive molecules. Normally, this involves analyzing how the designed sensor responds to different amounts of both specific and nonspecific molecules. We have assessed the sensitivity of the developed sensor toward vWFA2, a molecule of interest as a biomarker, by testing its reaction when mixed with interferon γ-induced protein 10 (IP-10) in the presence of bovine serum albumin (BSA). Though many immunogenic molecules are overexpressed in systemic inflammation, both vWFA2 and IP-10 are elevated in acute phase response in systemic inflammation, both vWFA2 and IP-10 are elevated in acute phase response.[28] To eliminate potential interference of IP-10 in real-time measurement, we measured the response of the sensor against BSA and IP-10. The biosensor signal measurement in the protein-rich environment is a noteworthy study to confirm the specificity of the sensor toward vWFA2. Evaluation was done by testing low and high concentrations of the specific as well as

https://doi.org/10.1021/acsmeasuresciau.4c00060
ACS Meas. Sci. Au 2024, 4, 721−728

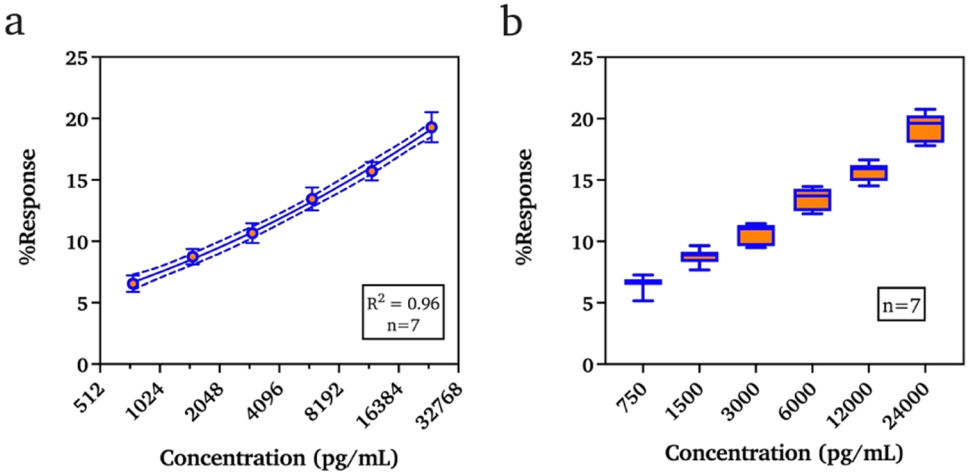

Figure 3. Regression analysis of the calibrated dose−response study (a); Box plot showing the distribution of calibrated dose response (b) for $n = 7$ electrodes.

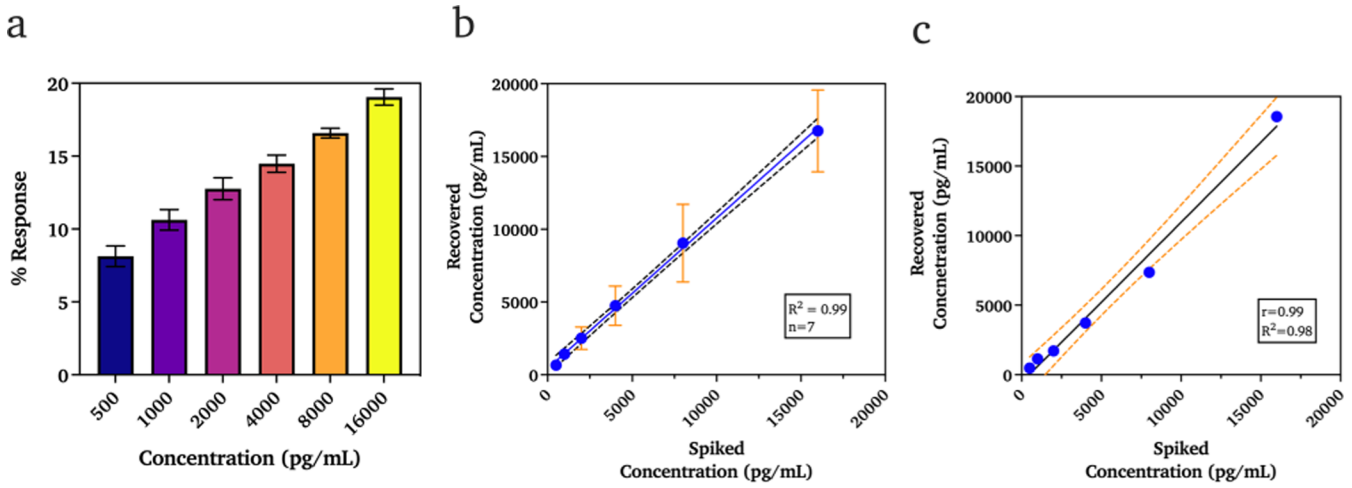

Figure 4. (a) Sensor response against different spiked concentrations; (b) Linear regression analysis of the spiked concentrations vs recovered concentrations ($n = 5$); (c) Pearson's correlation between spiked concentrations and recovered concentrations calculated using the calibrated dose−response curve.

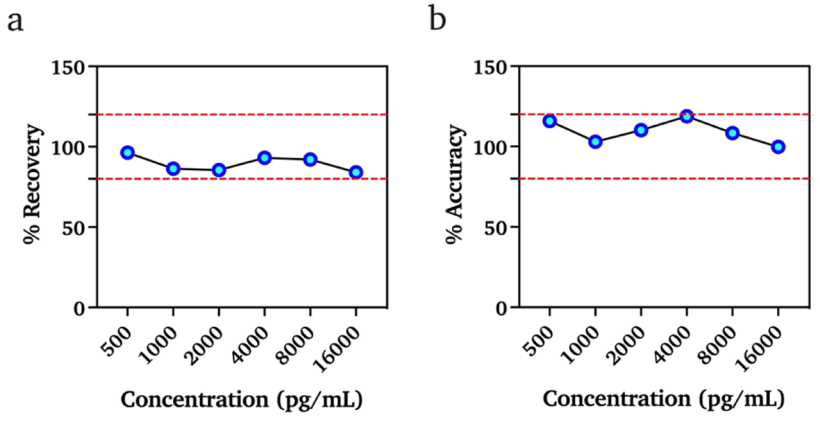

Figure 5. Percentage recovery (a) and percentage accuracy (b) calculated for the recovered concentrations using an established calibrated dose−response curve.

nonspecific molecules. Figure 6 displays the biosensor response achieved by the cross-reactivity study between vWFA2 and IP-10 and exemplifies a negligible cross-sensitivity. The results, depicted in Figure 6, indicate that there is minimal cross-reactivity between vWFA2 and IP-10. Specifically, the response to the nonspecific molecule (IP-10) at both low and high concentrations was found to be less than 20%, as depicted by the dotted line. Conversely, the response to the specific molecule (vWFA2) at both low and high concentrations was

https://doi.org/10.1021/acsmeasuresciau.4c00060
ACS Meas. Sci. Au 2024, 4, 721−728

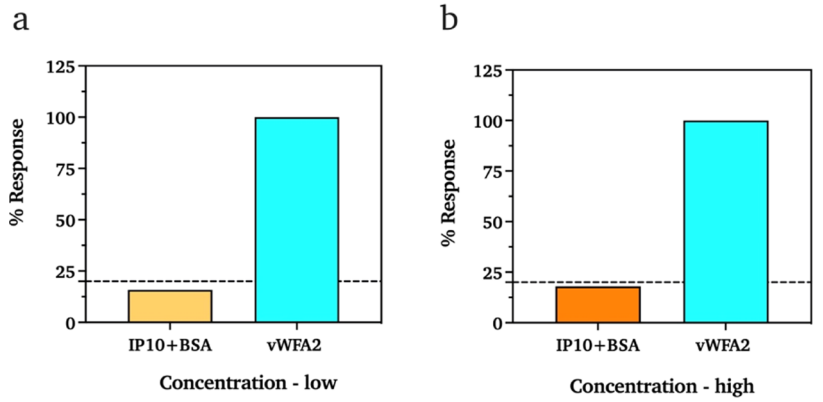

Figure 6. Biosensor response against cross-reactive molecule (IP-10) in the presence of BSA and vWFA2 at low (a) and high (b) concentrations.

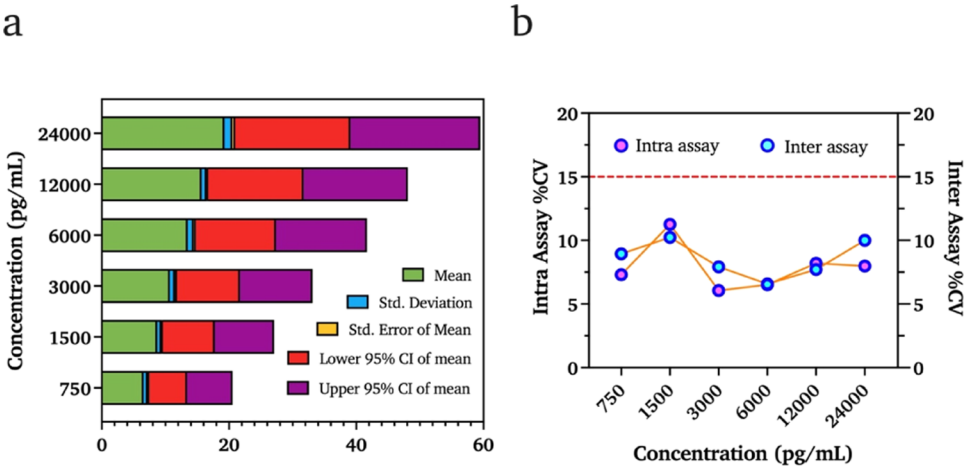

Figure 7. (a, b) Intra-assay variability (left *y*-axis) and Interassay variability (right *y*-axis) of the developed biosensor for various concentrations of vWFA2.

above 80%, demonstrating the sensor's specificity for the vWFA2 molecule in the presence of a nonspecific molecule.

A descriptive statistical analysis was conducted on the calibrated dose−response data to assess the variability in sensor performance across the vWFA2 ranges from 750 to 24,000 pg/mL (Table S2). Figure 7a depicts the statistical representation of the data, showing the percentage response for the mean value, along with the standard deviation and standard error of the mean. The figure also displays the lower and upper limits with 95% confidence intervals, confirming the biosensor's ability to detect vWFA2 with minimal deviation from the average for $n = 7$ sensors. In addition to assessing the accuracy and specificity of the biosensor, we have evaluated the other biosensor parameters such as repeatability and reproducibility. Biosensors were assessed for variation within an electrode for multiple measurements (intra-assay) and between electrodes (interassay). The intra-assay study (Figure 7b, left-handed *y*-axis) showed a %CV range of 6.05 to 11.26%, while the interassay study (Figure 7b, right-handed *y*-axis) showed a %CV range of 6.57 to 10.23% (Table S3). Both results fall within the ideal clinical threshold of a %CV < 20%, demonstrating the accuracy, specificity, repeatability, and reproducibility of the biosensor platform within the sensor.

The sensor's accuracy was confirmed by calculating the percentage of recovery and accuracy. Different concentrations of vWFA2 (500, 1000, 2000, 4000, 8000, and 16,000 pg/mL) were added to pooled plasma, and sensor response was measured (Table S1). Concentrations were estimated using the calibrated dose−response curve and percentage recovery was calculated and shown in Figure 5a. vWFA2 in plasma showed a recovery percentage ranging from 84 to 100%, which falls within the ideal biosensor range. The accuracy of the biosensors was also important to establish to ensure sensor efficacy. As shown in Figure 5b, six different concentrations of vWFA2 diluted in pooled plasma were tested using the electrochemical device. The calculated recovered concentrations showed that the sensor was within 86−110% accuracy in predicting the unknown concentrations, demonstrating its ability to accurately detect vWFA2 molecules spiked onto the plasma samples, as shown in Figure 5b. This percentage of accuracy range confirms the sensor's ability to accurately detect the vWFA2 molecules that were spiked onto the plasma samples.

CONCLUSIONS AND FUTURE PERSPECTIVES

In this research, we successfully functionalized the biosensor surface with the DTSSP cross-linker and vWFA2 antibody, enabling the detection of the vWFA2 antigen. This point-of-care biosensing device could specifically detect vWFA2 proteins in blood plasma in a short testing time and using a small sample volume. It had a wide linear range of detection from 750 to 24,000 pg/mL for vWFA2 and showed a good correlation in estimating unknown spiked concentrations in pooled plasma. The biosensor's precision, accuracy, and

https://doi.org/10.1021/acsmeasuresciau.4c00060
ACS Meas. Sci. Au 2024, 4, 721−728

specificity were evaluated and confirmed, indicating its effectiveness in the proposed biofluid. These findings highlight the importance of monitoring vWFA2 levels, a protein involved in the interplay between inflammatory and coagulatory systemic states, to provide a comprehensive understanding of a patient's inflammatory status. Monitoring levels of these inflammatory biomarkers is crucial for making treatment decisions for patients who may progress to a critically ill state. In the future, this biomolecular sensor can be continuously monitored to determine a full range of clinical manifestations. The developed point-of-care biosensing platform for detecting inflammatory biomarkers has the potential to revolutionize detection and diagnosis mechanisms in various inflammatory and infectious diseases.

■ ASSOCIATED CONTENT

Data Availability Statement

All the data generated or analyzed during this study are included in this article and its Supporting Information files.

Supporting Information

The Supporting Information is available free of charge at https://pubs.acs.org/doi/10.1021/acsmeasuresciau.4c00060.

Response of vWF to endothelial injury by mediating the adhesion between platelets and subendothelial components at sites of vascular damage; depicts the schematic representation of vWF binding to injured vascular subendothelial cells through specific glycoprotein receptor interactions (S.Figure 1); spiked concentrations were compared against recovered concentrations, and biosensor recovery rates (S.Table 1); descriptive statistical analysis of the biosensor response to different vWFA2 concentrations (S.Table 2); inter and intra assay variability of the biosensor response to different vWFA2 concentrations (S.Table 3) (PDF)

■ AUTHOR INFORMATION

Corresponding Author

Shalini Prasad − *Department of Bioengineering, The University of Texas at Dallas, Richardson, Texas 75248, United States;* orcid.org/0000-0002-2404-3801; Email: Shalini.prasad@utdallas.edu

Authors

Bianca Elizabeth David − *Department of Bioengineering, The University of Texas at Dallas, Richardson, Texas 75248, United States*

Sasya Madhurantakam − *Department of Bioengineering, The University of Texas at Dallas, Richardson, Texas 75248, United States*

Jayanth Babu Karnam − *EnLiSense LLC, Allen, Texas 75013, United States*

Sriram Muthukumar − *EnLiSense LLC, Allen, Texas 75013, United States;* orcid.org/0000-0002-8761-7278

Complete contact information is available at: https://pubs.acs.org/10.1021/acsmeasuresciau.4c00060

Author Contributions

§B.E.D. and S.M. contributed equally to this work. CRediT: **Bianca Elizabeth David** data curation, formal analysis, writing - original draft; **Sasya Madhurantakam** conceptualization, data curation, formal analysis, methodology, validation, writing - original draft, writing - review & editing; **jayanth babu karnam** formal analysis, resources, writing - review & editing; **Sriram Muthukumar** conceptualization, data curation, funding acquisition, investigation, project administration, resources, supervision, writing - review & editing; **Shalini Prasad** conceptualization, funding acquisition, investigation, methodology, project administration, resources, supervision, writing - review & editing.

Notes

The authors declare the following competing financial interest(s): S.P. and S.M. have a significant interest in EnLiSense LLC, a company that may have a commercial interest in the results of this research and technology. The potential individual conflict of interest has been reviewed and managed by The University of Texas at Dallas and played no role in the study design; in the collection, analysis, and interpretation of data; in the writing of the report, or in the decision to submit the report for publication.

■ REFERENCES

(1) Gragnano, F.; Sperlongano, S.; Golia, E.; Natale, F.; Bianchi, R.; Crisci, M.; Fimiani, F.; Pariggiano, I.; Diana, V.; Carbone, A.; Cesaro, A.; Concilio, C.; Limongelli, G.; Russo, M.; Calabrò, P. The Role of von Willebrand Factor in Vascular Inflammation: From Pathogenesis to Targeted Therapy. *Mediators Inflammation* **2017**, *2017*, No. 5620314.

(2) Brun-Buisson, C. The Epidemiology of the Systemic Inflammatory Response. *Intensive Care Med.* **2000**, *26*, S064−S074, DOI: 10.1007/S001340051121.

(3) Davies, M. G.; Hagen, P. O. Systemic Inflammatory Response Syndrome. *J. Br. Surg.* **2005**, *84* (7), 920−935.

(4) Asimakopoulos, G. Mechanisms of the Systemic Inflammatory Response. *Perfusion* **1999**, *14* (4), 269−277.

(5) Weigand, M. A.; Hörner, C.; Bardenheuer, H. J.; Bouchon, A. The Systemic Inflammatory Response Syndrome. *Best Pract. Res. Clin. Anaesthesiol.* **2004**, *18* (3), 455−475.

(6) Levi, M.; van Der Poll, T.; Büller, H. R. Bidirectional Relation between Inflammation and Coagulation. *Circulation* **2004**, *109* (22), 2698−2704.

(7) Gebauer, J. M.; Flachsenberg, F.; Windler, C.; Richer, B.; Baumann, U.; Seeger, K. Structural and Biophysical Characterization of the Type VII Collagen VWFA2 Subdomain Leads to Identification of Two Binding Sites. *FEBS Open Bio* **2020**, *10* (4), 580−592.

(8) Meyer, D.; Girma, J. P. Von Willebrand Factor: Structure and Function. *Thromb. Haemostasis* **1993**, *70* (1), 99−104.

(9) McGrath, R. T.; McRae, E.; Smith, O. P.; O'Donnell, J. S. Platelet von Willebrand Factor − Structure, Function and Biological Importance. *Br. J. Hamaetol.* **2010**, *148* (6), 834−843.

(10) Haberichter, S. L.; Castaman, G.; Budde, U.; Peake, I.; Goodeve, A.; Rodeghiero, F.; Federici, A. B.; Batlle, J.; Meyer, D.; Mazurier, C.; Goudemand, J.; Eikenboom, J.; Schneppenheim, R.; Ingerslev, J.; Vorlova, Z.; Habart, D.; Holmberg, L.; Lethagen, S.; Pasi, J.; Hill, F. G. H.; Montgomery, R. R. Identification of Type 1 von Willebrand Disease Patients with Reduced von Willebrand Factor Survival by Assay of the VWF Propeptide in the European Study: Molecular and Clinical Markers for the Diagnosis and Management of Type 1 VWD (MCMDM-1VWD). *Blood* **2008**, *111* (10), 4979−4985.

(11) Voorberg, J.; Fontijn, R.; Van Mourik, J. A.; Pannekoek, H. Domains Involved in Multimer Assembly of von Willebrand Factor (VWF): Multimerization Is Independent of Dimerization. *EMBO J.* **1990**, *9* (3), 797−803.

(12) Lynch, C. J.; Lane, D. A.; Luken, B. M. Control of VWF A2 Domain Stability and ADAMTS13 Access to the Scissile Bond of Full-Length VWF. *Blood* **2014**, *123* (16), 2585−2592.

(13) Leineweber, S.; Schönig, S.; Seeger, K. Insight into Interactions of the Von-Willebrand-Factor-A-like Domain 2 with the FNIII-like Domain 9 of Collagen VII by NMR and SPR. *FEBS Lett.* **2011**, *585* (12), 1748−1752.
(14) Zhang, Q.; Zhou, Y. F.; Zhang, C. Z.; Zhang, X.; Lu, C.; Springer, T. A. Structural Specializations of A2, a Force-Sensing Domain in the Ultralarge Vascular Protein von Willebrand Factor. *Proc. Natl. Acad. Sci. U.S.A.* **2009**, *106* (23), 9226−9231.
(15) Ansar, W.; Ghosh, S.Inflammation and Inflammatory Diseases, Markers, and Mediators: Role of CRP in Some Inflammatory Diseases. In *Biology of C Reactive Protein in Health and Disease*; Springer, 2016; pp 67−107.
(16) Cortes, G. A.; Moore, M. J.; El-Nakeep, S. *Physiology, Von Willebrand Factor*; StatPearls Publishing, 2024.
(17) Kawecki, C.; Lenting, P. J.; Denis, C. V. Von Willebrand Factor and Inflammation. *J. Thromb. Haemostasis* **2017**, *15* (7), 1285−1294.
(18) Ruggeri, Z. M. Von Willebrand Factor. *J. Clin. Invest.* **1997**, *99* (4), 559−564.
(19) Berntorp, E. Erik von Willebrand. *Thromb. Res.* **2007**, *120*, S3−S4.
(20) Hotchkiss, R. S.; Karl, I. E. The Pathophysiology and Treatment of Sepsis. *N. Engl. J. Med.* **2003**, *348* (2), 138−150.
(21) Madhurantakam, S.; Lee, Z. J.; Naqvi, A.; Karnam, J. B.; Muthukumar, S.; Prasad, S. Multiplex Sensing of IL-10 and CRP towards Predicting Critical Illness in COVID-19 Infections. *Biosens. Bioelectron.: X* **2023**, *13*, No. 100307.
(22) Tanak, A. S.; Muthukumar, S.; Krishnan, S.; Schully, K. L.; Clark, D. V.; Prasad, S. Multiplexed Cytokine Detection Using Electrochemical Point-of-Care Sensing Device towards Rapid Sepsis Endotyping. *Biosens. Bioelectron.* **2021**, *171*, No. 112726.
(23) Madhurantakam, S.; Karnam, J. B.; Dhamu, V. N.; Seetaraman, S.; Gates-Hollingsworth, M. A.; AuCoin, D. P.; Clark, D. V.; Schully, K. L.; Muthukumar, S.; Prasad, S. Electrochemical Immunoassay for Capturing Capsular Polysaccharide of Burkholderia Pseudomallei: Early Onsite Detection of Melioidosis. *ACS Infect. Dis.* **2024**, *10* (6), 2118−2126.
(24) Madhurantakam, S.; Karnam, J. B.; Muthukumar, S.; Prasad, S. COVID Severity Test (CoST Sensor)—An Electrochemical Immunosensing Approach to Stratify Disease Severity. *Bioeng. Transl. Med.* **2023**, *8*, No. e10566, DOI: 10.1002/btm2.10566.
(25) Tripathy, N.; Kim, D. H. Metal Oxide Modified ZnO Nanomaterials for Biosensor Applications. *Nano Converg.* **2018**, *5* (1), No. 27.
(26) Tanak, A. S.; Jagannath, B.; Tamrakar, Y.; Muthukumar, S.; Prasad, S. Non-Faradaic Electrochemical Impedimetric Profiling of Procalcitonin and C-Reactive Protein as a Dual Marker Biosensor for Early Sepsis Detection. *Anal. Chim. Acta: X* **2019**, *3*, No. 100029.
(27) Upasham, S.; Prasad, S. Tuning SLOCK toward Chronic Disease Diagnostics and Management: Label-Free Sweat Interleukin-31 Detection. *ACS Omega* **2021**, *6* (31), 20422−20432.
(28) Madhurantakam, S.; Lee, Z. J.; Naqvi, A.; Prasad, S. Importance of IP-10 as a Biomarker of Host Immune Response: Critical Perspective as a Target for Biosensing. *Curr. Res. Biotechnol.* **2023**, *5*, No. 100130.

https://doi.org/10.1021/acsmeasuresciau.4c00060
ACS Meas. Sci. Au 2024, 4, 721−728